

Supporting Information for

**A Fast and Selective Near-Infrared Fluorescent Sensor for Multicolor Imaging of
Biological Nitroxyl (HNO)**

Alexandra T. Wrobel, Timothy C. Johnstone, Alexandria Deliz-Liang, Stephen J. Lippard*,
and Pablo Rivera-Fuentes*.

Department of Chemistry, Massachusetts Institute of Technology, Cambridge, Massachusetts
02139, United States

*lippard@mit.edu
*priveraf@mit.edu

Contents

Figure S1. ^1H NMR spectrum (500 MHz, $\text{DMSO-}d_6$) of 3 at 20 °C.	3
Figure S2. $^{13}\text{C}\{^1\text{H}\}$ NMR spectrum (125 MHz, $\text{DMSO-}d_6$) of 3 at 20 °C.	3
Figure S3. ^1H NMR spectrum (500 MHz, $\text{DMSO-}d_6$) of DHX1 at 20 °C.	4
Figure S4. $^{13}\text{C}\{^1\text{H}\}$ NMR spectrum (125 MHz, $\text{DMSO-}d_6$) of DHX1 at 20 °C.	4
Figure S5. COSY spectrum (500 MHz, $\text{DMSO-}d_6$) of DHX1 at 20 °C.	5
Figure S6. Analytical HPLC traces of 3 and DHX1.	5
Figure S7. High resolution ESI-MS of Cu- 3 bearing a CF_3COO^- ligand.	6
Figure S8. High resolution ESI-MS of CuDHX1 bearing a CF_3COO^- ligand.	6
Figure S9. Low resolution ESI-MS of CuDHX1 upon reaction with 100 equiv of Angeli's salt.	7
Figure S10. Low resolution ESI-MS of Cu- 3 upon reaction with 100 equiv of Angeli's salt.	7
Figure S11. Fluorescence spectra of Cu- 3 and after reaction with HNO and NO.	8
Figure S12. Photophysical properties of 3 and Cu- 3	8
Figure S13. Time dependent fluorescence experiments of CuDHX1 in aqueous buffer.	9
Figure S14. Time dependent fluorescence experiments of DHX1 in aqueous buffer.	9
Figure S15. Time dependent fluorescence experiments of CuDHX1 in CH_3OH	10
Figure S16. Selectivity of CuDHX1 in CH_3CN	10
Figure S17. pH profile of CuDHX1.	11
Figure S18. Cyclic voltammograms of CuDHX1, DHX1, and Cu(II)-cyclam.	12
Figure S19. Cyclic voltammogram of Cu- 3	12
Figure S20. Simulated EPR spectra.	13

Figure S21. EPR spectra of CuDHX1 prepared using CuCl ₂	13
Figure S22. EPR spectra of Cu-3.....	14
Figure S23. Cell imaging experiments in DMEM.....	14
Figure S24. Time-lapsed microscopy measurements.....	15
Figure S25. Cell imaging selectivity studies.	15
Figure S26. Selectivity of CuDHX1 in HeLa cells for HNO over H ₂ S.	16
Figure S27. Zinc induced fluorescence selectivity over NaNO ₂ and NaOH.....	16

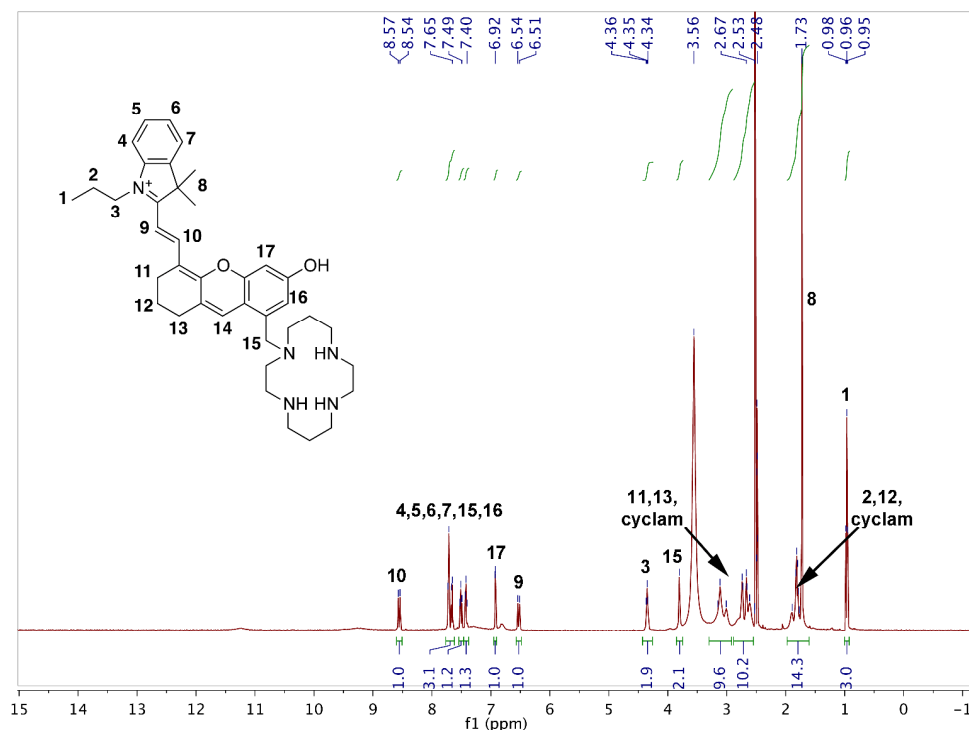


Figure S1. ^1H NMR spectrum (500 MHz, $\text{DMSO-}d_6$) of **3** at 20 °C. Assignment of representative peaks. The signals around 2.5 and 3.56 ppm correspond to residual DMSO and H_2O respectively.

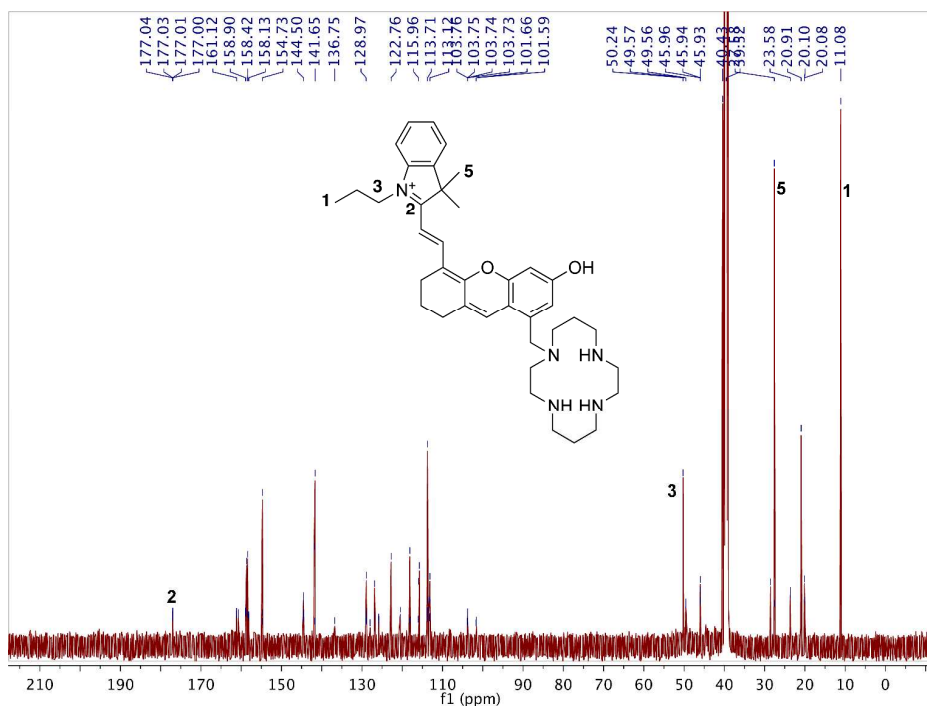


Figure S2. $^{13}\text{C}\{^1\text{H}\}$ NMR spectrum (125 MHz, $\text{DMSO-}d_6$) of **3** at 20 °C. Assignment of representative peaks. The signal around 39 ppm corresponds to DMSO.

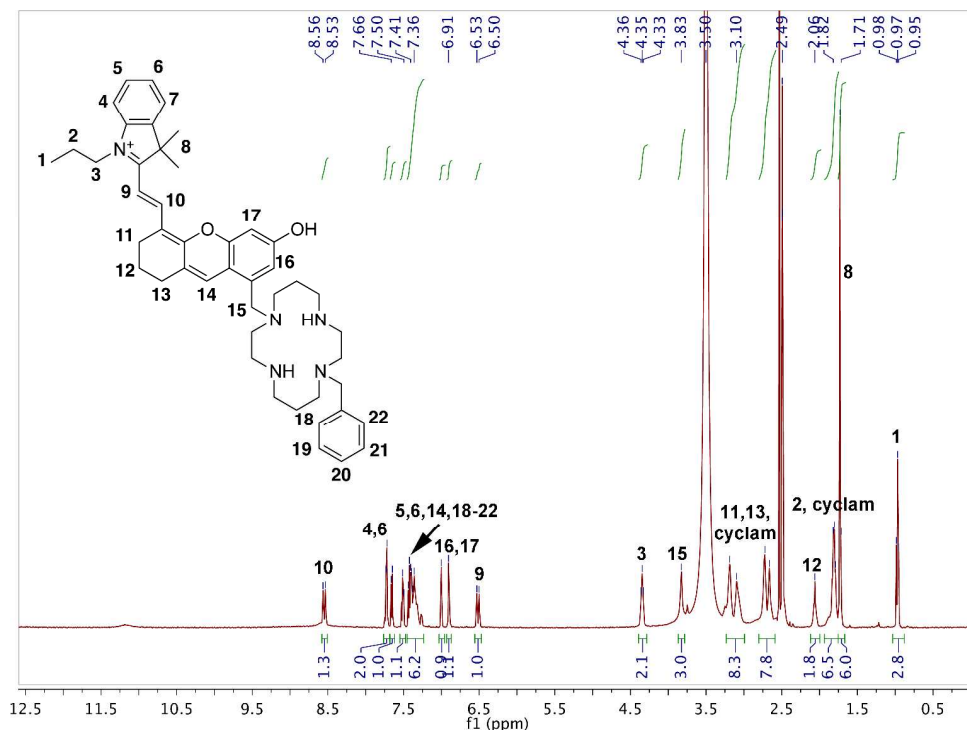


Figure S3. ^1H NMR spectrum (500 MHz, $\text{DMSO-}d_6$) of DHX1 at 20 °C. Assignment of representative peaks. The signals around 2.5 and 3.56 ppm correspond to residual DMSO and H_2O respectively.

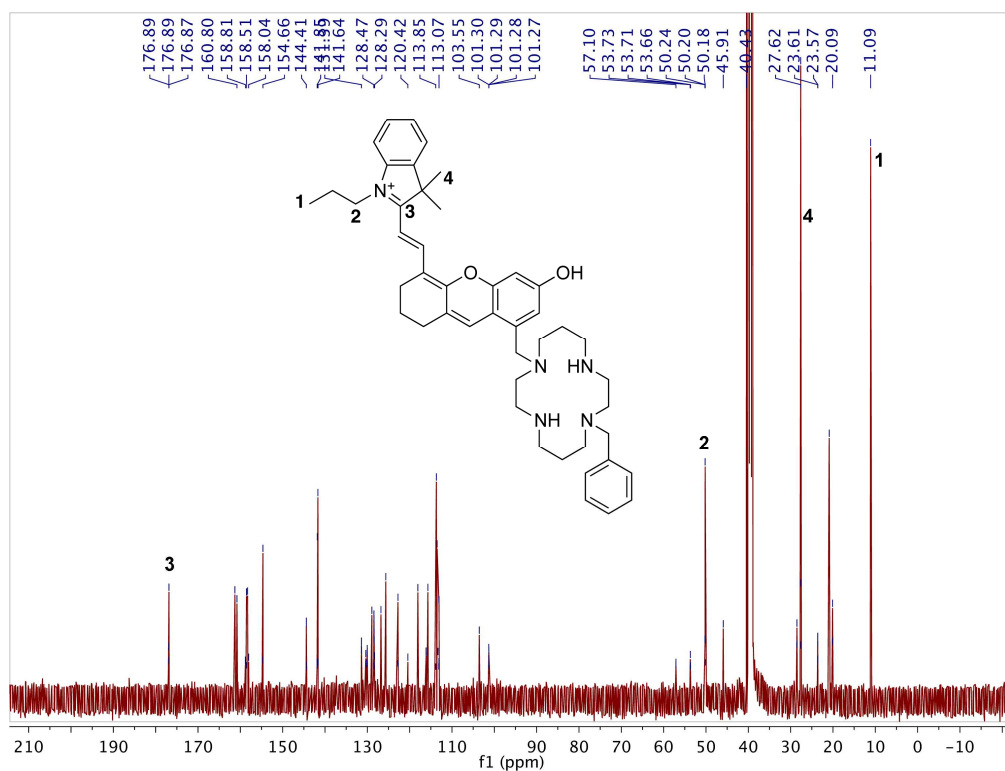


Figure S4. $^{13}\text{C}\{^1\text{H}\}$ NMR spectrum (125 MHz, $\text{DMSO-}d_6$) of DHX1 at 20 °C. Assignment of representative peaks. The signal around 39 ppm corresponds to residual DMSO.

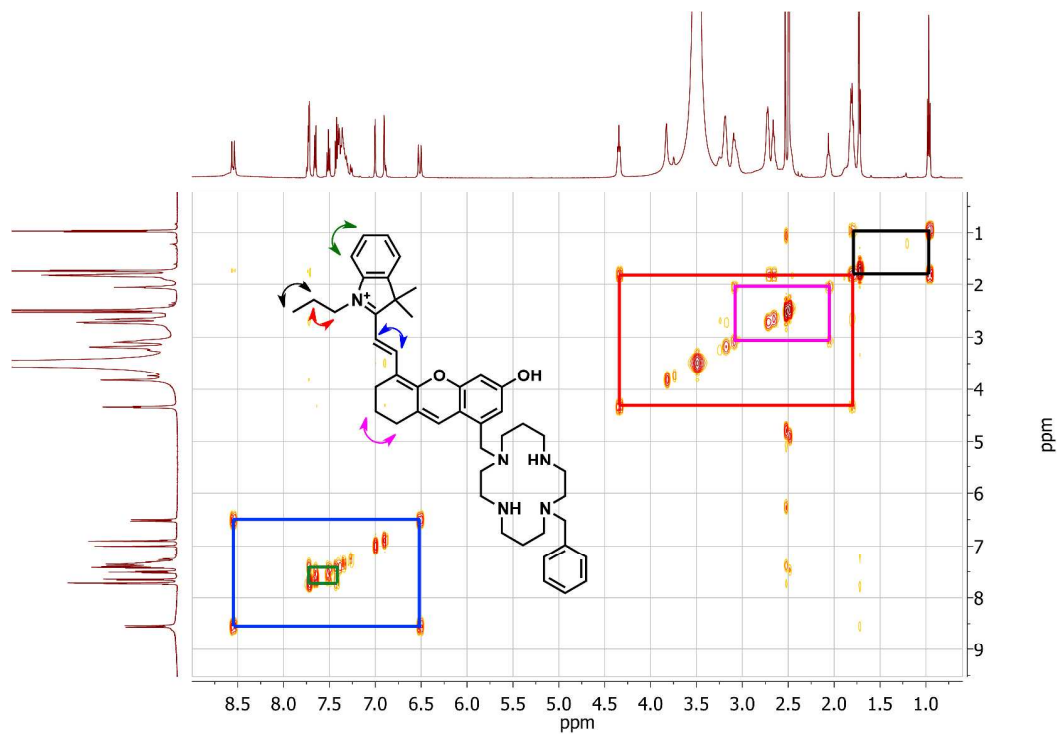


Figure S5. COSY spectrum (500 MHz, DMSO- d_6) of DHX1 at 20 °C. Cross-peaks that can be unambiguously assigned to specific $^3J_{\text{H-H}}$ couplings are shown in color.

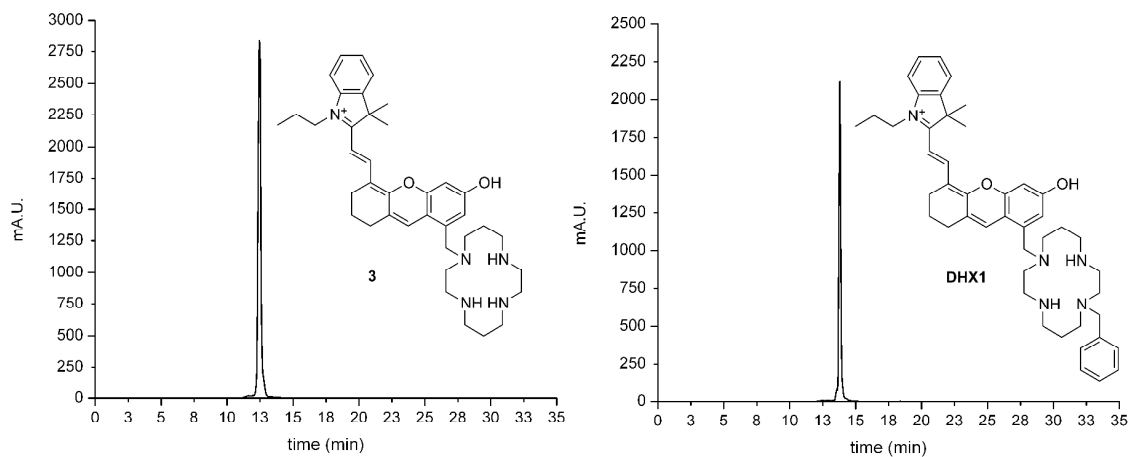


Figure S6. Analytical HPLC traces of **3** and DHX1. Detection wavelength: 650 nm.

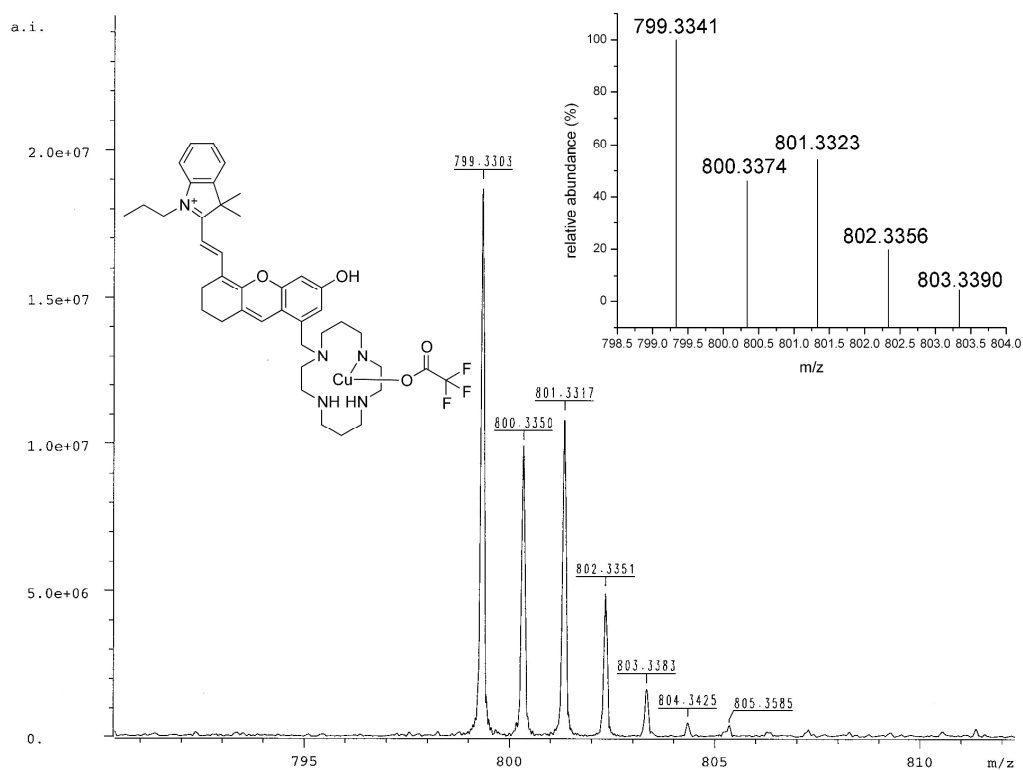


Figure S7. High resolution ESI-MS of Cu-3 bearing a CF_3COO^- ligand. The inset shows the calculated isotope distribution.

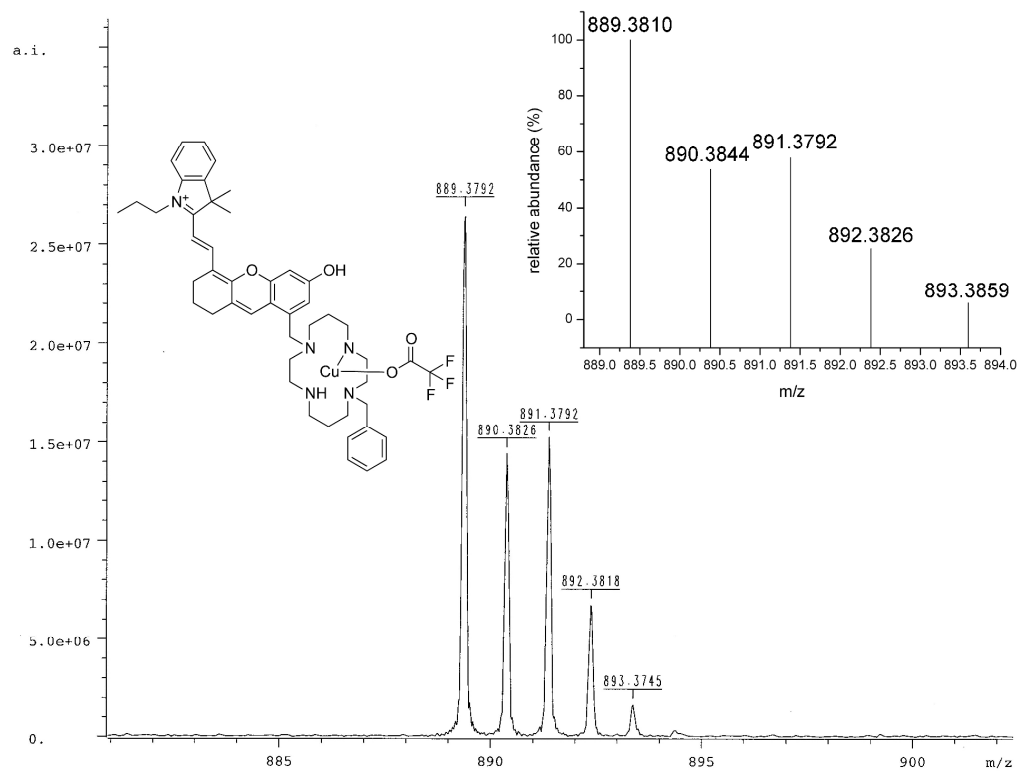


Figure S8. High resolution ESI-MS of CuDHX1 bearing a CF_3COO^- ligand. The inset shows the calculated isotope distribution.

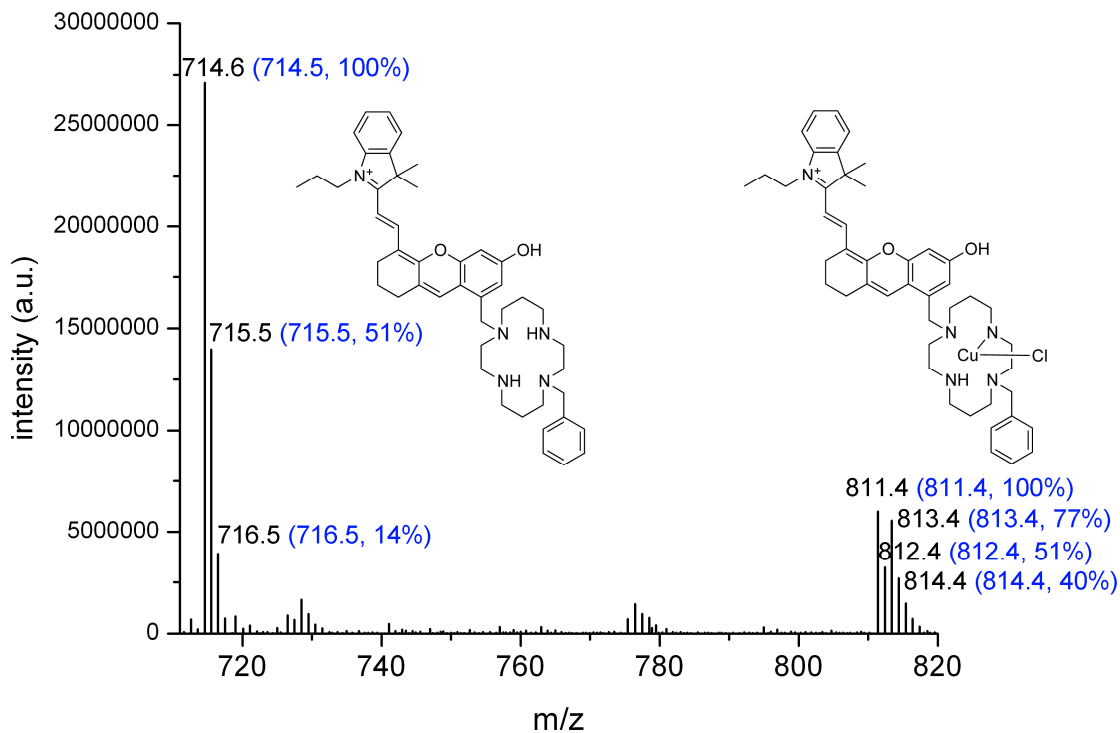


Figure S9. Low resolution ESI-MS of CuDHX1 upon reaction with 100 equiv of Angeli's salt. Calculated mass and relative abundances for the structures shown are given in parentheses.

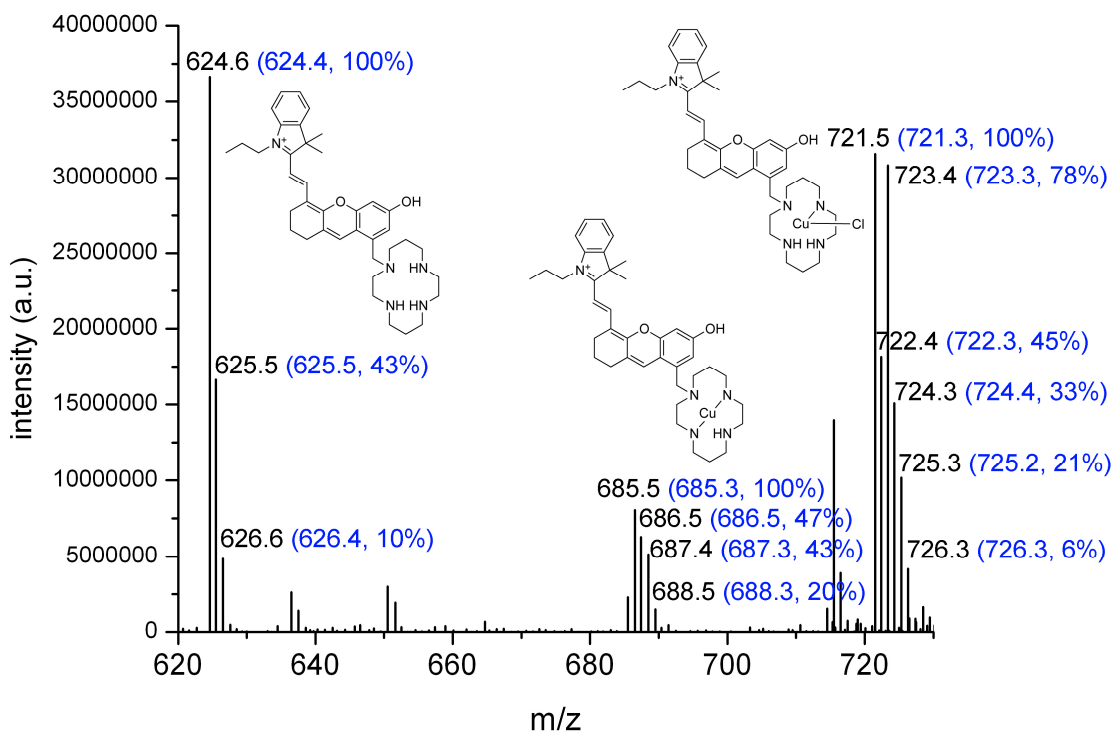


Figure S10. Low resolution ESI-MS of Cu-3 upon reaction with 100 equiv of Angeli's salt. Calculated mass and relative abundances for the structures shown are given in parenthesis.

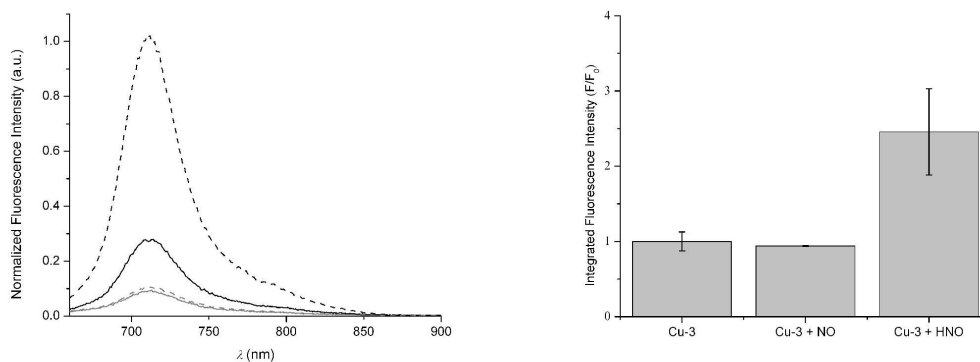


Figure S11. Fluorescence spectra of Cu-3 and after reaction with HNO and NO. Left: Fluorescence spectra of 5 μ M Cu-3 (grey solid line) in aqueous buffer (50 mM PIPES, 100 mM KCl, pH = 7) and 2 min after addition of 100 equiv of Angeli's salt (black solid line) or 5000 equiv of NO (grey dotted line), compared to ligand 3 (black dotted line). λ_{ex} : 650 nm. Right: Normalized integrated fluorescence intensity (660–900 nm) of the same experiment.

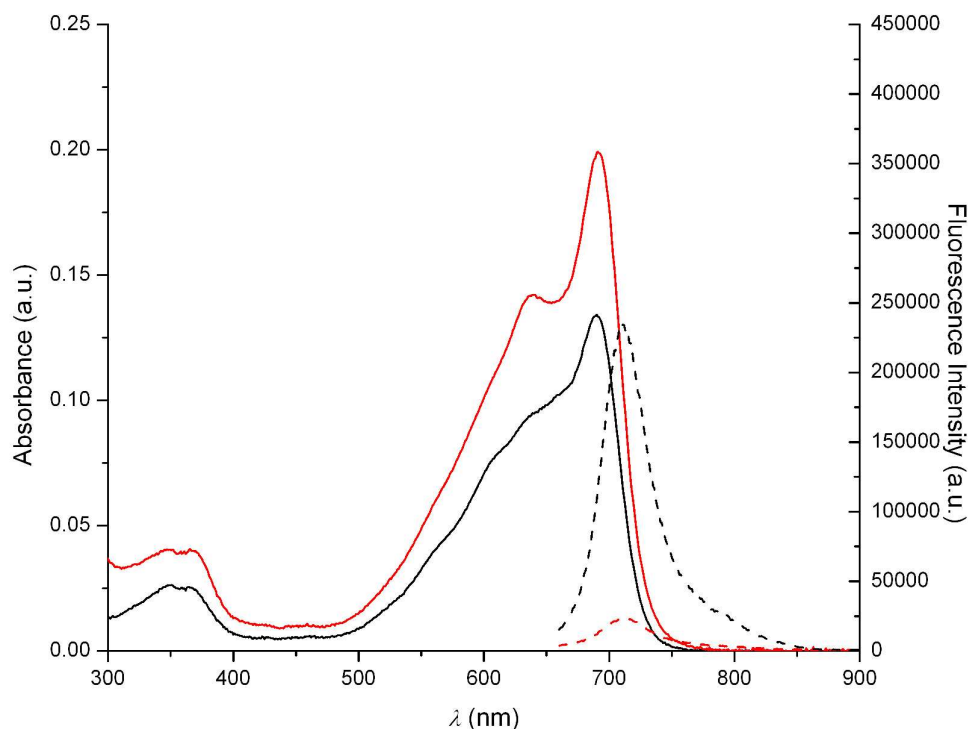


Figure S12. Photophysical properties of 3 and Cu-3. Fluorescence (dotted lines) and absorbance (solid lines) spectra of 3 (black) and Cu-3 (red) in aqueous buffer (50 mM PIPES, 100 mM KCl, pH = 7). λ_{ex} : 650 nm.

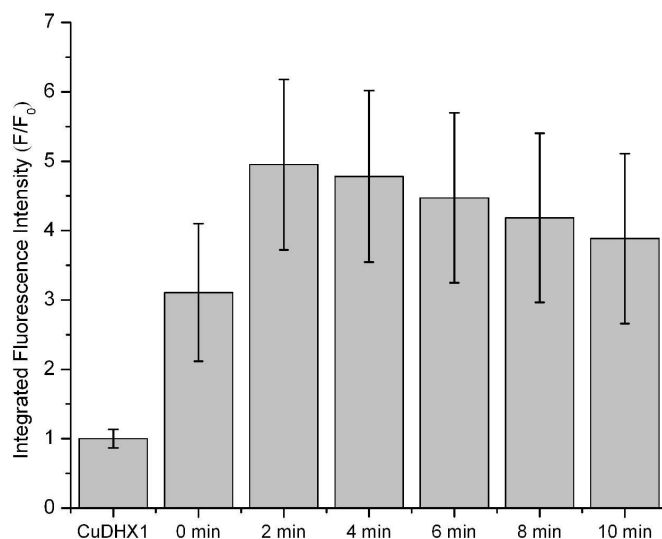


Figure S13. Time dependent fluorescence experiments of CuDHX1 in aqueous buffer. Time-dependent normalized integrated (660–900 nm) fluorescence intensity of 2 μ M CuDHX1 in aqueous buffer (50 mM PIPES, 100 mM KCl, pH = 7) after addition of 100 equiv of Angeli's salt. λ_{ex} : 650 nm.

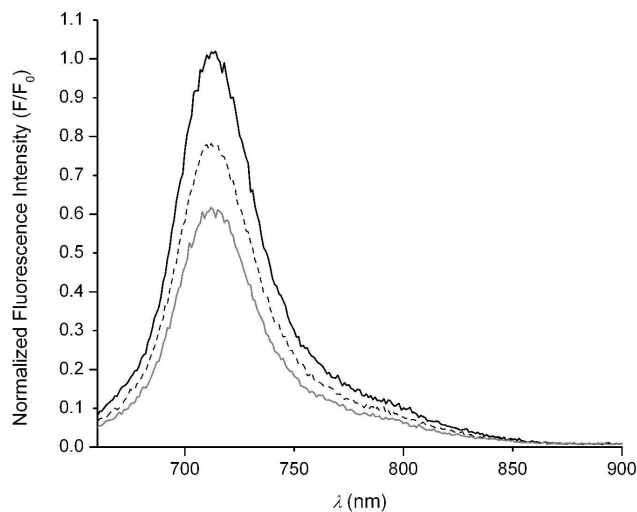


Figure S14. Time dependent fluorescence experiments of DHX1 in aqueous buffer. Time-dependent fluorescence spectra of 2 μ M DHX1 (black solid line) in aqueous buffer (50 mM PIPES, 100 mM KCl, pH = 7) and after addition of 100 equiv of Angeli's salt (0 min: black dotted line; 10 min: grey solid line). λ_{ex} : 650 nm.

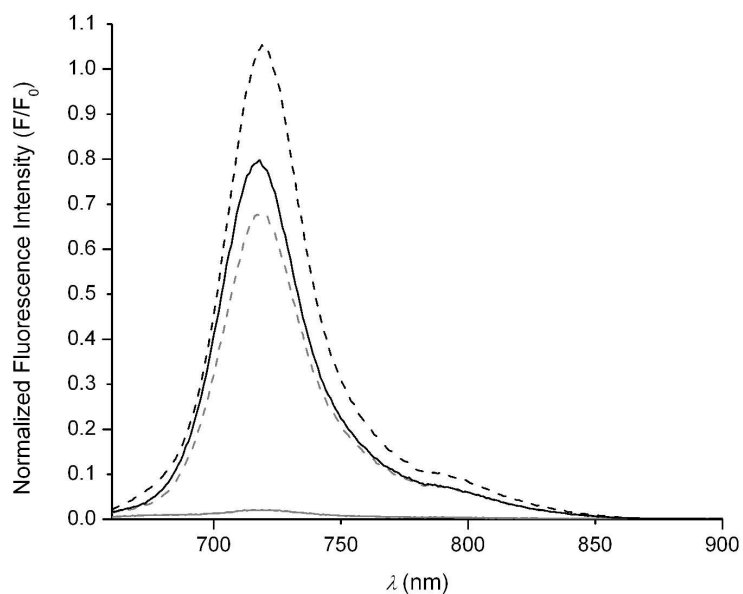


Figure S15. Time dependent fluorescence experiments of CuDHX1 in CH₃OH. Time-dependent fluorescence spectra of 2 μM CuDHX1 (grey solid line) in CH₃OH and after addition of 100 equiv of Angeli's salt (0 min: grey dotted line; 10 min: black solid line), compared to DHX1 (black dotted line). λ_{ex} : 650 nm.

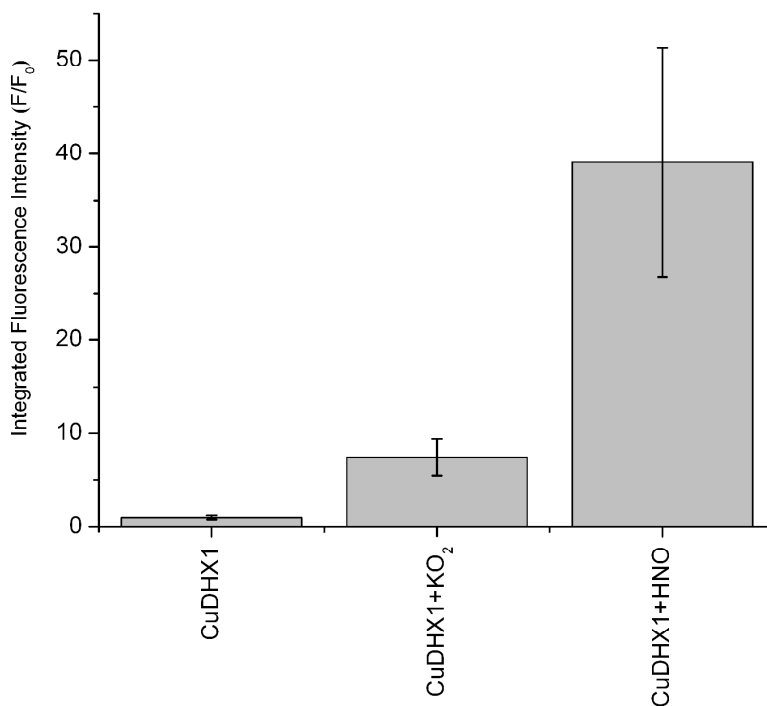


Figure S16. Selectivity of CuDHX1 in CH₃CN. Normalized integrated (660–900 nm) fluorescence intensity of 2 μM CuDHX1 in CH₃CN after addition of 100 equiv of Angeli's salt or KO₂. λ_{ex} : 650 nm.

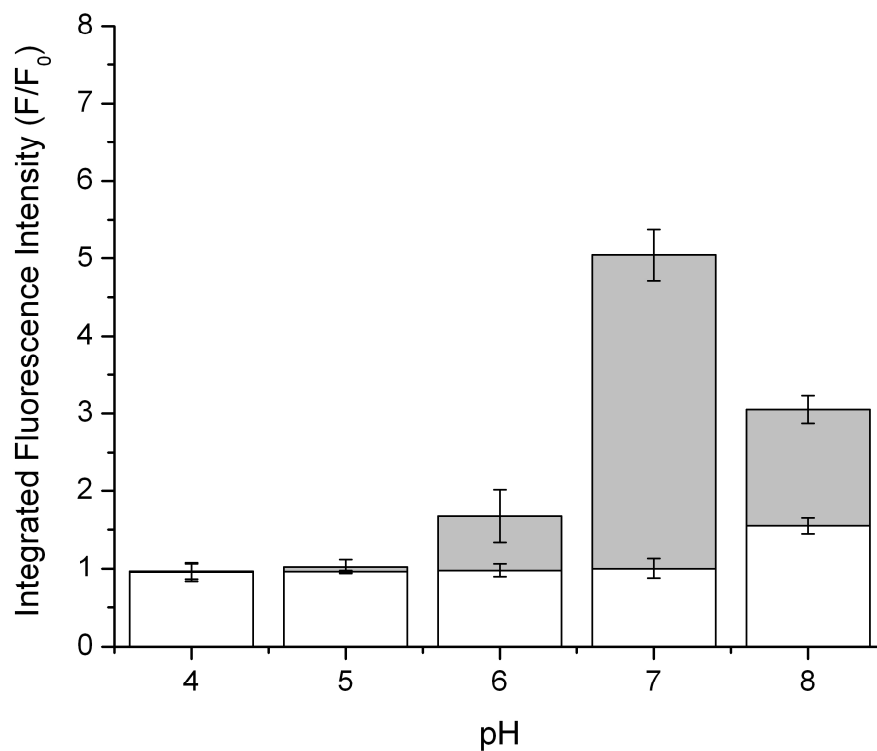


Figure S17. pH profile of CuDHX1.

Normalized integrated (660–900 nm) fluorescence intensity of 2 μM CuDHX1 in aqueous buffer (0.1 M MES, 100 mM KCl; pH 4 and 5 or 50 mM PIPES, 100 mM KCl; pH 6, 7, and 8) before (white bars) and after (grey bars) addition of 100 equiv of Angeli's salt. The intensities were normalized with respect to 2 μM CuDHX1 at pH 7 before addition of Angeli's salt. λ_{ex} : 650 nm.

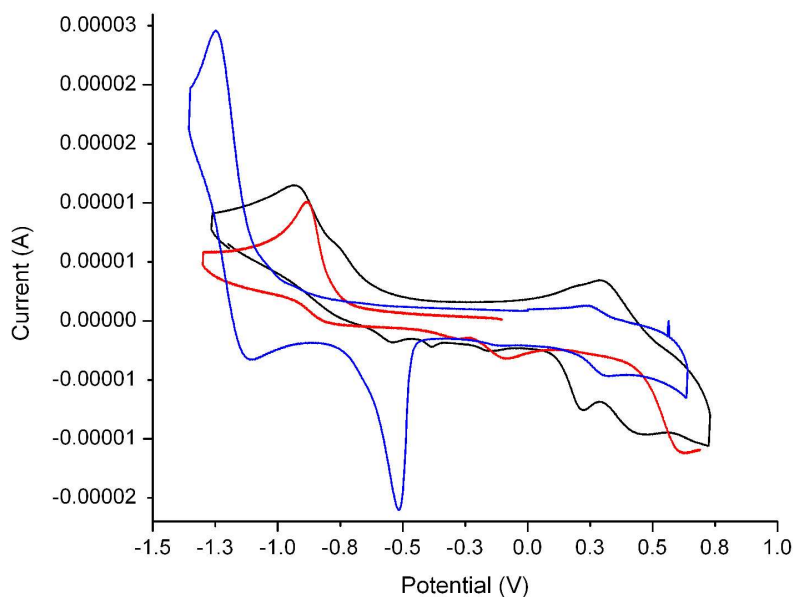


Figure S18. Cyclic voltammograms of CuDHX1, DHX1, and Cu(II)-cyclam. Cyclic voltammogram of 1 mM CuDHX1 (black), Cu(II)-cyclam (blue), and ligand DHX1 (red) in CH₃CN containing 0.1 M *n*-Bu₄NPF₆ as the supporting electrolyte, using a glassy carbon working electrode, Pt auxiliary electrode, and Ag pseudo reference electrode. Fc/Fc⁺ was used as internal standard. Cu(II)-cyclam and DHX1 were measured to assign the features in the voltammogram of CuDHX1.

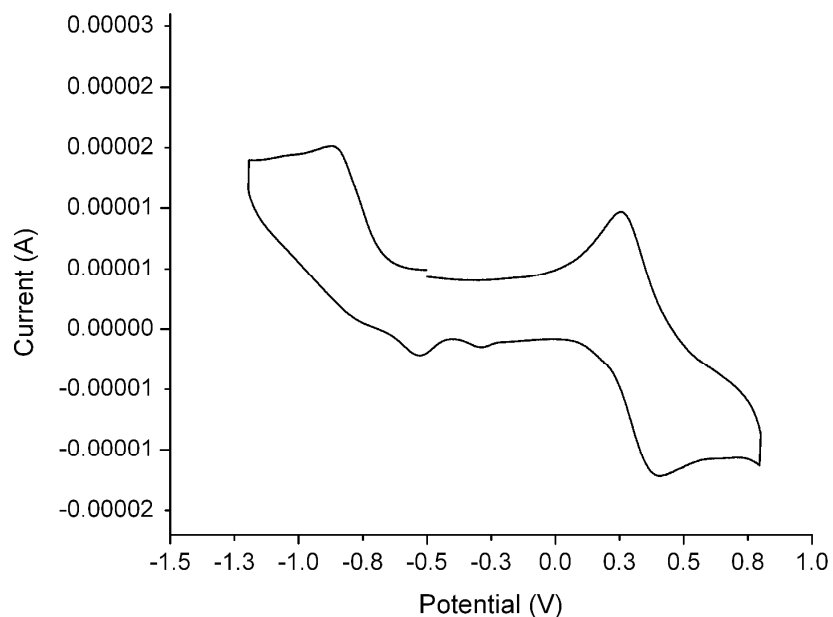


Figure S19. Cyclic voltammogram of Cu-3. Cyclic voltammogram of 1 mM Cu-3 in CH₃CN containing 0.1 M *n*-Bu₄NPF₆ as the supporting electrolyte, using a glassy carbon working electrode, Pt auxiliary electrode, and Ag pseudo reference electrode. Fc/Fc⁺ was used as internal standard.

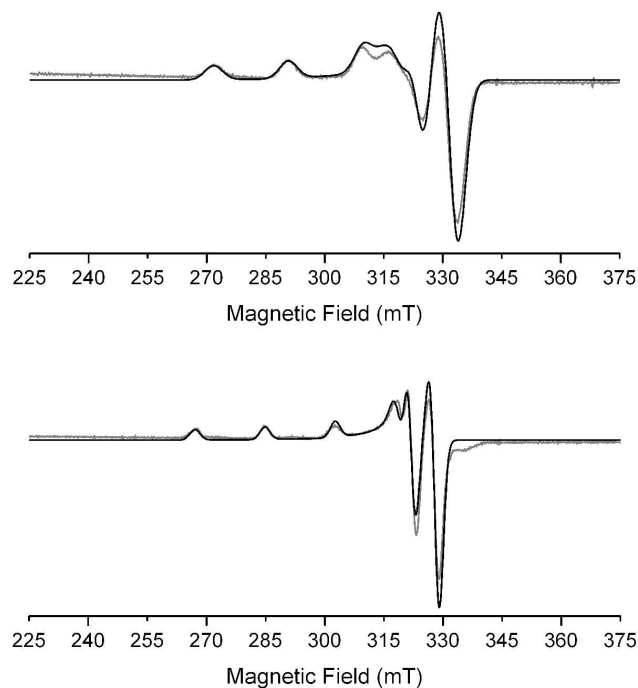


Figure S20. Simulated EPR spectra.

Overlay of experimental (grey) and simulated EPR spectra (black) (77 K) of 400 μM CuDHX1 (top) in CH_3OH and after addition of 100 equiv of Angeli's salt, followed by re-oxidation (bottom).

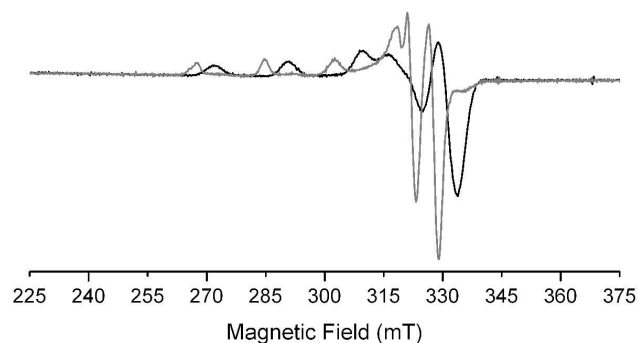


Figure S21. EPR spectra of CuDHX1 prepared using CuCl_2 .

X-band EPR spectra of 400 μM CuDHX1 (black) and after addition of 100 equiv Angeli's salt (grey) in CH_3OH . In this experiment, CuDHX1 was prepared using CuCl_2 under in air. This solution was degassed and the EPR tube was prepared under anaerobic conditions. Addition of Angeli's salt to this solution did not abolish the EPR signal, but instead gave a more axially symmetric signal assigned to a re-oxidation product, probably because of the presence of air or other oxidizing impurities in CuCl_2 . This experiment demonstrates that the reduced, EPR-silent derivative of CuDHX1 can only be observed when the sample is prepared and handled under strict anaerobic conditions.

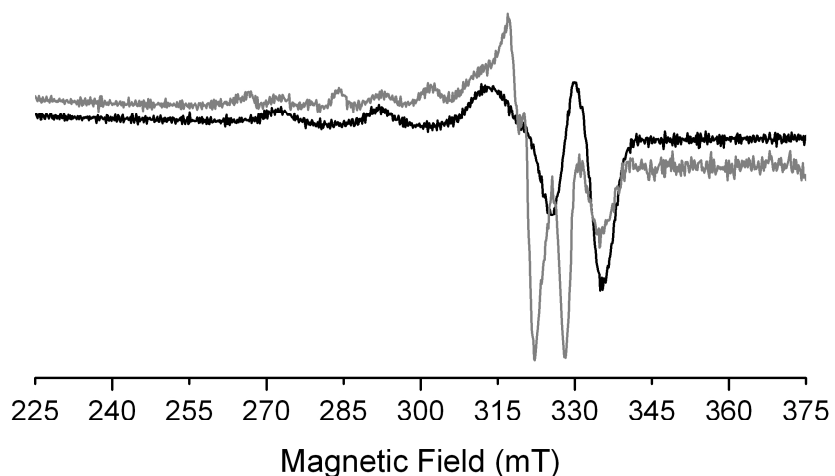


Figure S22. EPR spectra of Cu-3.

X-band EPR spectra of 400 μM Cu-3 (black) and after addition of 100 equiv Angeli's salt (grey) in CH_3OH . Even under strict anaerobic conditions, a reduced, EPR-silent derivative of Cu-3 could not be observed.

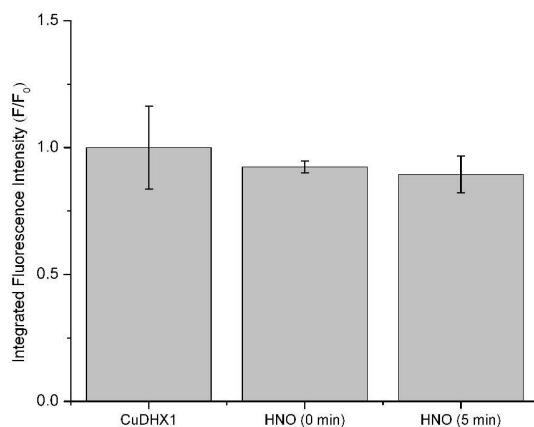


Figure S23. Cell imaging experiments in DMEM.

Time-dependent integrated fluorescence intensity (NIR channel) of HeLa cells incubated with 5 μM CuDHX1 in DMEM (10% FBS, 1% penicillin/streptomycin) and after addition of 300 equiv of Angeli's salt. The lack of turn-on response in DMEM could be because HNO can react with cysteine or other components of DMEM before it can enter the cell.

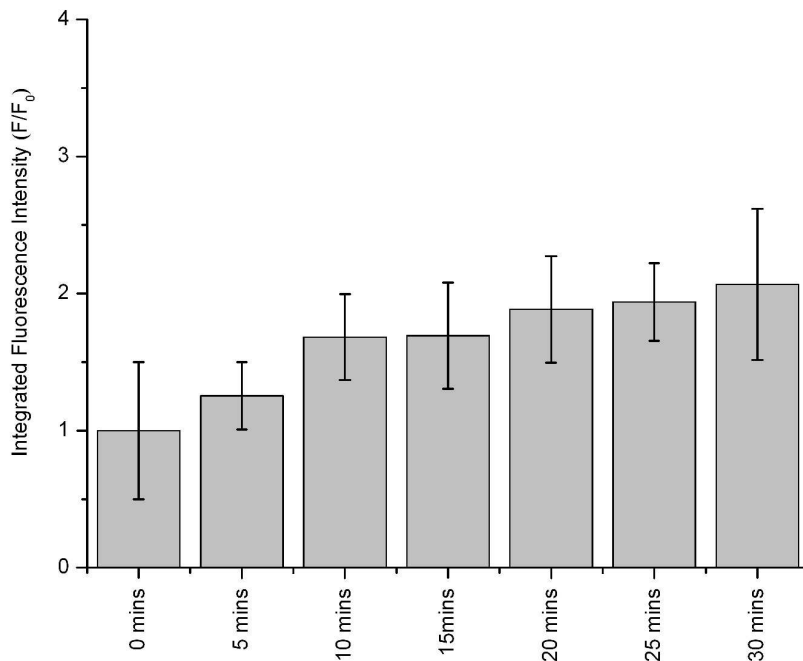


Figure S24. Time-lapsed microscopy measurements. Time-dependent increase in integrated fluorescence intensity (NIR channel) of HeLa cells incubated with 5 μ M CuDHX1 in PBS buffer.

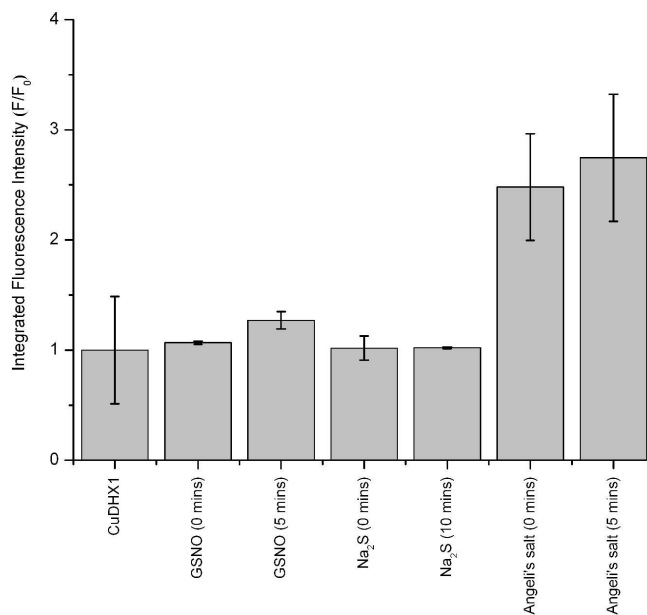


Figure S25. Cell imaging selectivity studies. Increase in integrated fluorescence intensity (NIR channel) of HeLa cells incubated with 5 μ M CuDHX1 in PBS before and after addition of 300 equiv of GSNO (NO donor), 300 equiv of Na₂S, or 300 equiv of Angeli's salt.

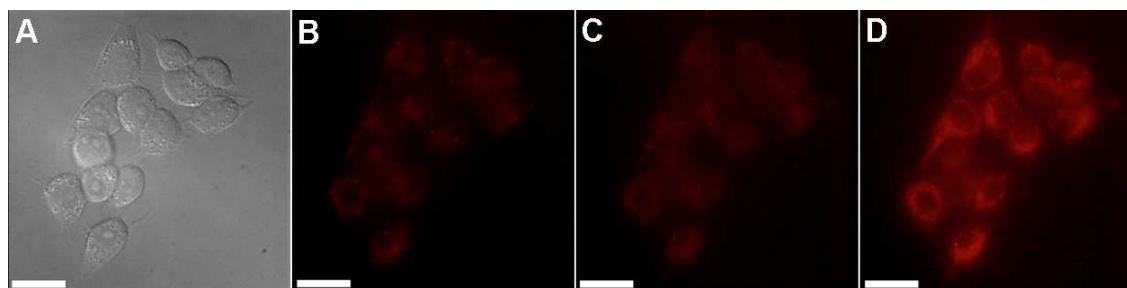


Figure S26. Selectivity of CuDHX1 in HeLa cells for HNO over H₂S.

A) Differential interference contrast (DIC) image, B) NIR channel before treatment with 1.5 mM Na₂S, (c) NIR channel 10 min after treatment with 1.5 mM Na₂S, (d) NIR channel 10 min treatment with 1.5 mM Angeli's salt. Cells were incubated with 5 μM CuDHX1 in PBS. Scale bar = 25 μm.

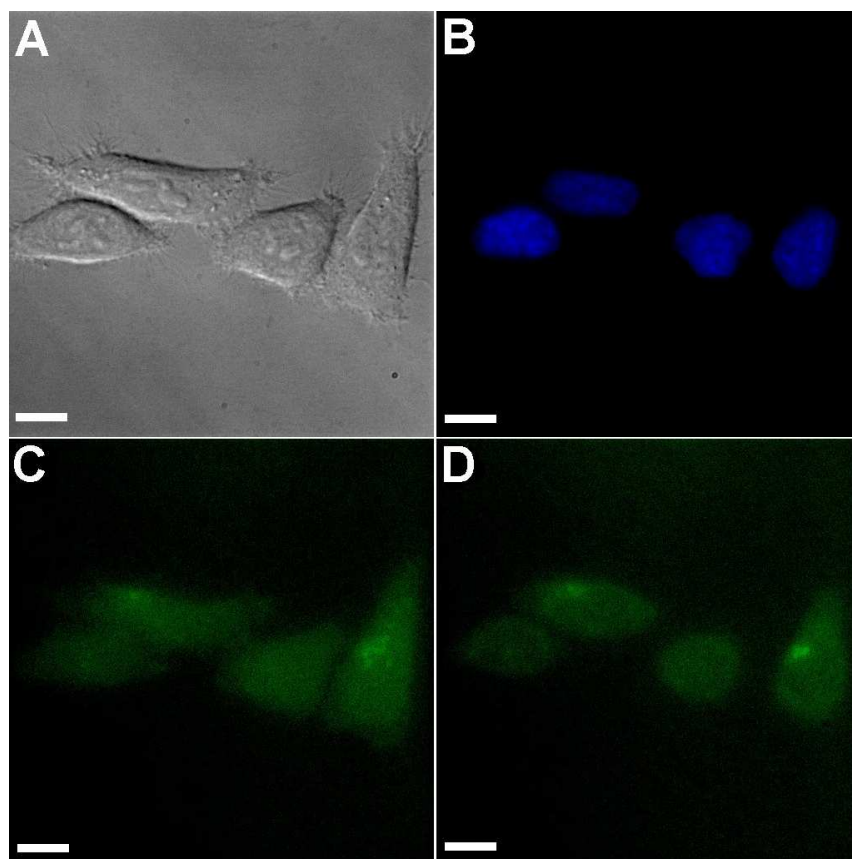


Figure S27. Zinc induced fluorescence selectivity over NaNO₂ and NaOH.

HeLa cells containing ZP1 and treated with 3 mM NaNO₂ in aqueous 10 mM NaOH. A) DIC image, B) Blue channel showing nuclei, C) Green channel before addition of NaNO₂, D) Green channel 20 min after treatment with 3 mM NaNO₂ in aqueous 10 mM NaOH. No significant change in fluorescence is observed in this experiment. Scale bar = 10 μm.